EDGE ARTICLE

Controlled scrambling reactions to polyphosphanes *via* bond metathesis reactions†

Robin Schoemaker,[a] Kai Schwedtmann,[a] Antonio Franconetti, [ID][b] Antonio Frontera, [ID][b] Felix Hennersdorf [ID][a] and Jan J. Weigand [ID] *[a]

Triphosphanes R′$_2$PP(R)PR′$_2$ (**9a,c**: R = Py; **9b** R = BTz), 1,3-diphenyl-2-pyridyl-triphospholane **9d** and pentaphospholanes (RP)$_5$ (**13**: R = Py; **18**: R = BTz) are obtained in high yield of up to 98% from the reaction of dipyrazolylphosphanes RPpyr$_2$ (**5**: R = Py; **6**: R = BTz; pyr = 1,3-dimethylpyrazolyl) and the respective secondary phosphane (R′$_2$PH, R′ = Cy (**9a,b**), ^{t}Bu (**9c**); PhPH(CH$_2$)$_2$PHPh (**9d**)). The formation of derivatives **9a–d** proceeds *via* a condensation reaction while the formation of **13** and **18** can only be explained by a selective scrambling reaction. We realized that the reaction outcome is strongly solvent dependent as outlined by the controlled scrambling reaction pathway towards pentaphospholane **13**. In our further investigations to apply these compounds as ligands we first confined ourselves to the coordination chemistry of triphosphane **9a** with respect to coinage metal salts and discussed the observation of different *syn*- and *anti*-isomeric metal complexes based on NMR and X-ray analyses as well as quantum chemical calculations. Methylation reactions of **9a** with MeOTf yield triphosphan-1-ium Cy$_2$MePP(Py)PCy$_2$$^+$ (**10**$^+$) and triphosphane-1,3-diium Cy$_2$MePP(Py)PMeCy$_2$$^{2+}$ (**11**$^{2+}$) cations as triflate salts. Salt **11**[OTf]$_2$ reacts with pentaphospholane **13** in an unprecedented chain growth reaction to give the tetraphosphane-1,4-diium triflate salt Cy$_2$MePP(Py)P(Py)PMeCy$_2$$^{2+}$ (**19**[OTf]$_2$) *via* a P–P/P–P bond metathesis reaction. The latter salt is unstable in solution and rearranges *via* a rare [1,2]-migration of the Cy$_2$MeP-group followed by the elimination of the triphosph-2-en-1-ium cation [Cy$_2$MePPPMeCy$_2$]$^+$ (**20**$^+$) to yield a novel 1,4,2-diazaphospholium salt (**21**[OTf]).

Introduction

A wide range of polyphosphorus compounds, comprising diverse bonding motifs, have been synthesised in the last few decades.[1,2] Many of the observed compounds are often found to be labile in solution and their rearrangement or decomposition reactions are discussed to proceed *via* intermolecular scrambling reactions.[3] Even though there are early reports on controlling such scrambling reactions,[4] the selective and high yielding synthesis of certain polyphosphanes is still difficult, hampering their subsequent chemistry. Besides classical approaches for the generation of P–P bonds such as salt metathesis reactions,[2a,b] dehalosilylation reactions[2c] or condensation reactions,[2d] our group focusses on the development of methodologies using tripyrazolylphosphane **1** or derivatives thereof (*vide infra*) as a P$_1$-building unit for P–P bond forming reactions *via* condensation or P–N/P–P bond

metathesis reactions (Scheme 1).[5,6] In this regard, the reaction of **1** with Cy$_2$PH to give triphosphane **2** or *iso*-tetraphosphane **3** depending on the applied stoichiometry has been reported.[5] The reaction of **1** with 1,2-bis(phenylphosphanyl)ethane yields hexaphosphane **4** in a sequence of condensation and P–N/P–P bond metathesis reactions, showing an example of a controlled scrambling reaction.[6] In our effort to further control these metathesis reactions and driven by our general interest in azole-

[a]Faculty of Chemistry and Food Chemistry, TU Dresden, Chair of Inorganic Molecular Chemistry, 01062 Dresden, Germany. E-mail: jan.weigand@tu-dresden.de

[b]Department of Chemistry, Universitat de Illes Balears, 07122 Palma de Mallorca, Spain

† Electronic supplementary information (ESI) available. CCDC 1950469–1950486. For ESI and crystallographic data in CIF or other electronic format see DOI: 10.1039/c9sc04501e

Scheme 1 Application of tripyrazolylphosphane **1** in P–P bond formation reactions; (i) 2 Cy$_2$PH, −2 pyrH, CH$_3$CN; (ii) 3 Cy$_2$PH, −3 pyrH, and CH$_3$CN; (iii) 5 PhPH(CH$_2$)$_2$PHPh, 4 Ppyr$_3$, −PhP(pyr)(CH$_2$)$_2$-P(pyr)Ph, −10 pyrH, CH$_3$CN.

and azine-substituted phosphanes, we explored the synthesis of phosphanes with a pyridyl- or benzothiazolyl-substituent bound to phosphorus *via* the carbon atom. This limits the number of P–N bound pyrazolyl-substituents and therefore the possible reaction pathways by P–N/P–P bond metathesis. For a better overview and in thought of a systematic approach we organised our general types of phosphanes with respect to their number of P–N bound substituents as type I to type IV (Scheme 2). In type I phosphanes all three substituents are bound *via* P–N bonds whereas a type II phosphane is defined by two P–N bonds and one P–C bond. This order is maintained in type III phosphanes with one P–N and two P–C bonds and is finalised in type IV phosphanes featuring only P–C bonds. Importantly, all substituents at the phosphorus atom have an additional sp² hybridised donor atom such as nitrogen, being essential as a further reaction or coordination site and for the possible formation of resonance stabilised reaction intermediates. In this contribution, we report the synthesis of the hitherto unknown type II phosphanes carrying either a pyridyl- or benzothiazolyl-substituent and their use for the generation of triphosphanes, a triphospholane and pentaphospholanes and selected one triphosphane to explore its coordination chemistry with respect to coinage metal salts.

Results and discussion

The targeted type II phosphanes are synthesised by the reaction of the dichlorophosphanes RPCl₂ (R = Py (**5**); R = BTz (**6**))[7,8] with two equivalents of 3,5-dimethyl-1-(trimethylsilyl)pyrazole (Scheme 3).[9] The released chloro(trimethyl)silane can be removed under reduced pressure after 16 hours and no further purification is necessary. Both phosphanes **7** and **8** are conveniently prepared on a multi gram scale in excellent yields (97% (**7**); 96% (**8**)). The ³¹P NMR spectra of the dipyrazolylphosphanes show a singlet resonance in each case (**7**: $\delta(P)$ = 44.8 ppm; **8**: $\delta(P)$ = 38.0 ppm) being significantly shifted to a higher field compared to the corresponding dichlorophosphanes (**5**: $\delta(P)$ = 138.7 ppm; **6**: $\delta(P)$ = 132.0 ppm). Suitable crystals for X-ray analysis of phosphanes **7** and **8** are obtained by slow vapour diffusion of *n*-pentane into a saturated CH₂Cl₂ solution of **7** and
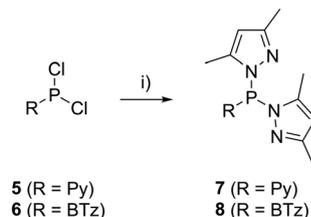
Scheme 3 Synthesis of dipyrazolylphosphanes **7** and **8**; R = Py; (i) 2 eq. pyrSiMe₃, neat, −2 Me₃SiCl; R = BTz; (i) 2 eq. pyrSiMe₃, Et₂O, −2 Me₃SiCl.

8. Their molecular structures are depicted in Fig. 1. The P–C bond lengths (**7**: P1–C1 1.827(1) Å; **8**: P1–C1 1.828(2) Å) are in the expected range of a P–C single bond (1.83 Å),[10] involving a tri-coordinate phosphorus atom. For both phosphanes the P–N bond lengths (**7**: P1–N4 1.721(1) Å, P1–N2 1.724(1) Å; **8** P1–N2/N2′ 1.719(1) Å) are in accordance with those reported for tri(1*H*-pyrazol-1-yl)phosphane (1.714(4) Å).[11] In continuation, we carried out the reaction of dipyrazolylphosphanes **7** and **8** with secondary phosphanes R′₂PH (R′ = Cy, *t*Bu or R′₂PH = PhP(H)C₂H₄P(H)Ph) to give triphosphanes **9a–c** and triphospholane **9d** with concomitant release of two equivalents of 3,5-dimethylpyrazole (Scheme 4). Compounds **9a–d** readily precipitate from the reaction mixture and are isolated by filtration. Subsequent washing with CH₃CN and drying *in vacuo* give **9a–d** as colourless solids in good to excellent yield (96% (**9a**); 93% (**9b**); 77% (**9c**); 69% (**9d**)). The ³¹P NMR spectra of all compounds show AX₂ spin systems which are characteristic of triphosphanes and 1,2,3-triphospholanes (Fig. 2). The NMR spectroscopic parameters are listed in Table 1. Single crystals for X-ray analysis are obtained by slow vapour diffusion of *n*-pentane into saturated CH₂Cl₂ solutions of **9a–d**. The molecular structures of **9a–d** are depicted in Fig. 3. Their structural parameters compare very well with those of similar triphosphanes[12] and are thus not discussed in detail. Only the bond angle of the P–P–P moiety in compound **9c** is approximately 10° wider which can be explained by the sterically demanding *tert*-butyl substituents. In recent years numerous examples of the coordination chemistry of anionic[13] and zwitterionic[14] oligophosphorus compounds towards transition metals have been
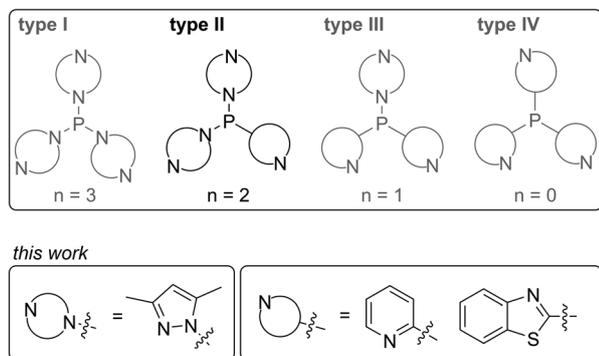
Scheme 2 Classification of *N*-heterocyclic substituted phosphanes into type I to type IV phosphanes (*n* is the number of P–N bonds) with an emphasis on the type II phosphanes presented in this contribution.
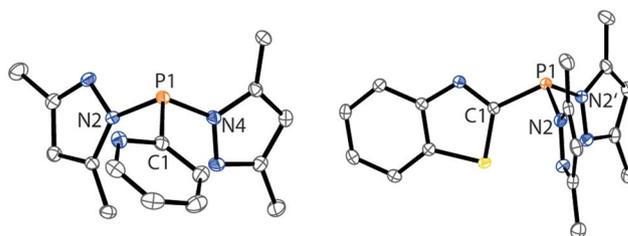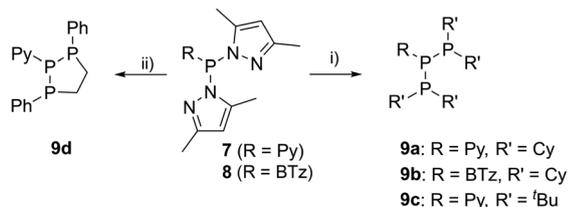

Fig. 1 Molecular structures of **7** (left) and **8** (right) (hydrogen atoms are omitted for clarity and thermal ellipsoids are displayed at 50% probability). Selected bond lengths (Å) and angles (°): (**7**) P1–C1 1.827(1), P1–N4 1.721(1), P1–N2 1.724(1), C1–P1–N4 101.28(5), N4–P1–N2 103.26(5), N2–P1–C1 100.18(5); (**8**) P1–C1 1.828(2), P1–N2 1.719(1), C1–P1–N2 101.26(5), N2–P1–N2′ 103.84(7).

Scheme 4 Synthesis of triphosphanes **9a–c**: (i) +2 eq. R′₂PH, CH_3CN, −2 pyrH; and triphospholane **9d**: (ii) 1 eq. $PhPH(CH_2)_2PHPh$, CH_3CN, −2 pyrH.
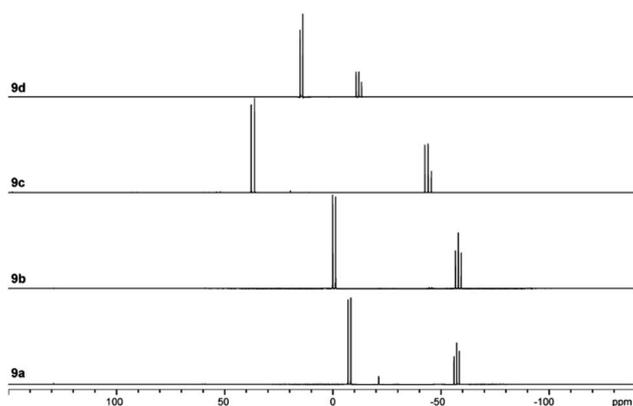

Fig. 2 ³¹P NMR spectra of compounds **9a–d**.

Table 1 ³¹P NMR parameters of compounds **9a–d**

| Compound	Chemical shifts (ppm)		$^1J_{PP}$ (Hz)
9a	−57.3	−7.7	−251
9b	−58.1	−0.7	−268
9c	−44.1	37.0	−307
9d	−12.1	14.5	−260

reported. Also, few examples of neutral triphosphanes coordinated to transition metals are known, however, the triphosphane moiety was assembled while coordinated to at least one metal centre.[15] Starting from stable triphosphanes only two complexes coordinating to metal carbonyls have been structurally characterised (Scheme 5, top),[5,16] while another example is described in solution.[17] In complex **I**, the triphosphane ligand chelates the $W(CO)_4$ moiety while in complex **II** the coordination of the $Fe(CO)_4$ moiety proceeds only *via* the free electron pair of one of the dicylcohexylphosphanyl groups. Featuring an additional nitrogen based donor site we envisioned the formation of multi-dentate coinage metal complexes using triphosphane **9a**, exemplarily. This yielded the first triphosphane coordination complexes of Cu(I), Ag(I) and Au(I) (Scheme 5). Reacting **9a** with an equimolar amount of Ag[OTf] in fluorobenzene at room temperature leads to the formation of a colourless precipitate which is isolated by filtration to yield the dinuclear complex [(**9a***Ag)₂][OTf]₂ in essentially quantitative yield. The corresponding reaction of **9a** with [(MeCN)₄Cu][OTf] in CH_2Cl_2 gives colourless plates upon slow vapour diffusion of *n*-pentane at −30 °C which can be isolated as [(**9a***Cu)₂][OTf]₂ up to a yield of 94%. Further transmetallation reaction of [(**9a***Ag)₂][OTf]₂ with (tht)AuCl in MeCN gives [(**9a***Au)₂][OTf]₂ in 64% yield by the concomitant precipitation of AgCl. Slow diffusion of *n*-pentane into a CH_2Cl_2 solution of **9a** and [(MeCN)₄Cu][OTf] in a 2 : 1 ratio gives crystalline [(**9a**)₂*Cu][OTf] in 93% yield. Formation of (**9a***CuBr)₂ is achieved by slow diffusion of *n*-pentane into a THF solution of equimolar amounts of **9a** and (tht)CuBr. The molecular structures of the aforementioned coinage metal complexes are shown in Fig. 4 and the structural parameters are summarised in Table 2. Different from the known coordination motifs for **I** and **II**, the molecular structures of [(**9a***Cu)₂][OTf]₂, [(**9a***Ag)₂][OTf]₂ and [(**9a***Au)₂][OTf]₂ reveal dinuclear metal complexes featuring two triphosphane ligands. In addition to the terminal coordinating phosphorus atoms, the nitrogen atoms of the pyridyl-substituents are involved in the coordination resulting in an approximately tetrahedral coordination environment of the respective metal centre. While the molecular structures of the dinuclear complexes [(**9a***Cu)₂][OTf]₂ and [(**9a***Ag)₂][OTf]₂ reveal an *anti*-arrangement with inversion symmetry, the gold complex [(**9a***Au)₂][OTf]₂ crystallises as a centro-symmetrical *syn*-isomer. The inversion process within the complexes has
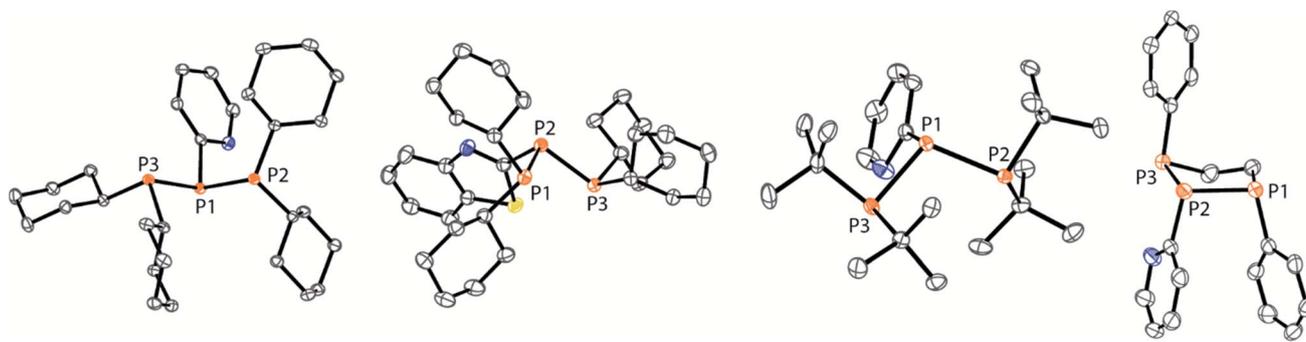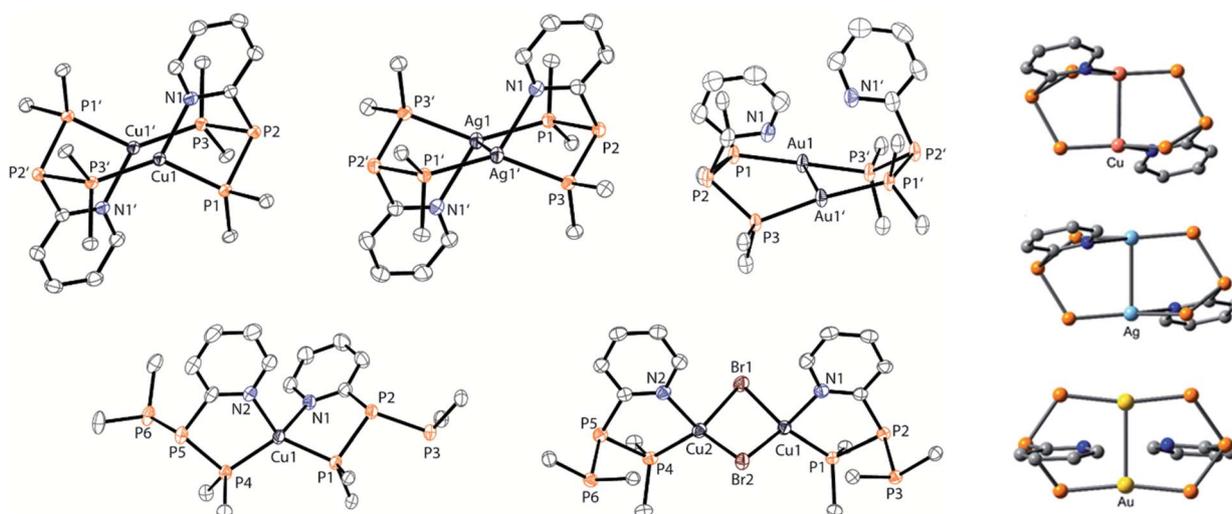

Fig. 3 Molecular structures of triphosphanes **9a–c** and triphospholane **9d** (hydrogen atoms are omitted for clarity and thermal ellipsoids are displayed at 50% probability). Selected bond lengths (Å) and angles (°) (**9a**): P1–P2 2.2301(3), P1–P3 2.2371(3), P3–P1–P2 97.38(1) (**9b**); P1–P2 2.2377(5), P2–P3 2.2234(5), P1–P2–P3 98.11(2) (**9c**); P1–P2 2.2181(3), P1–P3 2.2485(3), P2–P1–P3 107.64(1) (**9d**); P1–P2 2.270(2), P2–P3 2.197(2), P1–P2–P3 97.16(6).

Known triphosphanes coordinating to metal carbonyls
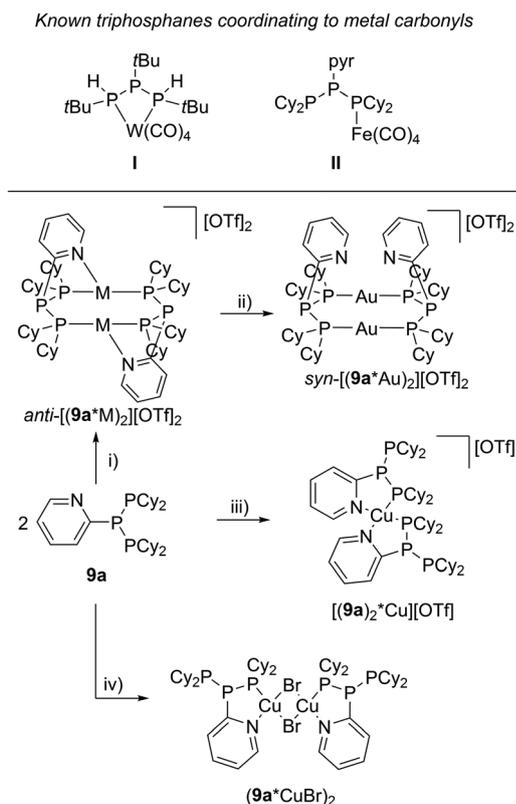
Scheme 5 Known transition metal complexes featuring a neutral triphosphane ligand (top); synthesis of coinage metal coordination complexes starting from triphosphane **9a** (bottom); (i) 2 eq. Ag[OTf], PhF (M = Ag); 2 eq. [(MeCN)$_4$Cu][OTf], CH$_2$Cl$_2$, −8 MeCN (M = Cu); (ii) 2 eq. (tht)AuCl, MeCN, −2 tht, −2 AgCl; (iii) 1 eq. [(MeCN)$_4$Cu][OTf], CH$_2$Cl$_2$, −4 MeCN; (iv) 2 eq. (tht)CuBr, THF, −2 tht.

been investigated by variable temperature NMR experiments and theoretical calculations (*vide infra*). The difference in the arrangement in the solid state causes a widening of the P–M–P angles in the copper complex [(**9a***Cu)$_2$][OTf]$_2$ (P3′-Cu1-P1 136.52(2)°) compared to the silver complex [(**9a***Ag)$_2$][OTf]$_2$ (P1–Ag1–P3′ 143.96(3)°) to an almost linear geometry around the gold atoms in [(**9a***Au)$_2$][OTf]$_2$ (P1–Au1–P3′ 171.52(3)°). The distances between the silver atoms in [(**9a***Ag)$_2$][OTf]$_2$ and the gold atoms in [(**9a***Au)$_2$][OTf]$_2$ indicate the presence of argentophilic and aurophilic interactions, respectively.[18] As the distance between the copper atoms in [(**9a***Cu)$_2$][OTf]$_2$ is slightly larger than the sum of the van der Waals radii of two copper atoms (2.80 Å),[19] significant van der Waals interactions can be excluded. The observed P–M bond lengths in [(**9a***M)$_2$] [OTf]$_2$ as well as in [(**9a**)$_2$*Cu][OTf] and (**9a***CuBr)$_2$ are in good agreement with bond lengths reported for the structurally similar [M$_2$(dcpm)$_2$]$^{2+}$ cations (M = Cu(ɪ), Ag(ɪ) or Au(ɪ); dcpm = bis(dicylcohexylphosphanyl)methane).[20] For (**9a***CuBr)$_2$ the formation of the typical Cu$_2$X$_2$ (X = halogen) geometry is found, only marginally differing from the typical planar arrangement reported for many Cu$_2$X$_2$-type structures.[21] Compared to free ligand **9a**, the P–P bond lengths and the P–P–P angles in the coinage metal complexes are only marginally altered. The room temperature NMR spectra of the dinuclear complexes [(**9a***Au)$_2$] [OTf]$_2$ and [(**9a***Ag)$_2$][OTf]$_2$ show broadened resonances due to dynamic processes in solution.[22] The low temperature ^{31}P NMR spectrum of [(**9a***Au)$_2$][OTf]$_2$ shows two separate AA′XX′X″X‴ spin systems at $\delta(P_A) = −34.2$ ppm, $\delta(P_X) = 52.6$ ppm and $\delta(P_A) = −37.8$ ppm, $\delta(P_X) = 50.3$ ppm corresponding to the respective *syn-* and *anti-*isomers (Fig. 5). Details of the coupling constants are included in the ESI.† For [(**9a***Ag)$_2$][OTf]$_2$ two isomers with two separate AA′XX′X″X‴ spin systems at $\delta(P_A) = −48.5$ ppm, $\delta(P_X) = 36.1$ ppm and $\delta(P_A) = −51.5$ ppm, $\delta(P_X) = 36.1$ ppm are

Fig. 4 Molecular structures of the coinage metal complexes [(**9a***Cu)$_2$][OTf]$_2$, [(**9a***Ag)$_2$][OTf]$_2$, [(**9a***Au)$_2$][OTf]$_2$, [(**9a**)$_2$*Cu][OTf] and (**9a***CuBr)$_2$ (hydrogen atoms, anions and solvate molecules are omitted for clarity, cyclohexyl groups are represented only by their phosphorus bound carbon atoms, and thermal ellipsoids are displayed at 50% probability; left). Selected geometrical parameters are given in Table 2; Optimised geometries of [(**9a***M)$_2$][OTf]$_2$ using the BP86-D3/def2-TZVP functional, showing the different coordination arrangement of the pyridyl-moieties towards the metal atoms (M = Cu, Ag, and Au; right).

Table 2 Selected geometrical parameters of crystallographically characterised coinage metal complexes [(9a*Cu)₂][OTf]₂, [(9a*Ag)₂][OTf]₂, [(9a*Au)₂][OTf]₂, [(9a)₂*Cu][OTf] and (9a*CuBr)₂

	[(9a*Cu)₂][OTf]₂	[(9a*Ag)₂][OTf]₂	[(9a*Au)₂][OTf]₂	[(9a)₂*Cu][OTf]^a	(9a*CuBr)₂^a
M1–M1′ in Å	2.8225(5)	2.9013(4)	2.880(3)	—	2.942
M1–P1 in Å	2.2755(4)	2.3818(8)	2.3033(8)	2.243	2.191
M1–P3′ in Å	2.2176(5)	2.4468(7)	2.3198(8)		
M–N in Å	2.048(1)	2.404(3)	2.948(3)	2.106	2.116
P–P^a in Å	2.225	2.224	2.226	2.212	2.214
P1-M1-P3 in °′	136.52(2)	143.96(3)	171.52(3)	—	—
P–P–P in °	98.26(2)	100.16(4)	98.29(5)	104.43	102.43

^{a} Average bond lengths and angles are given.
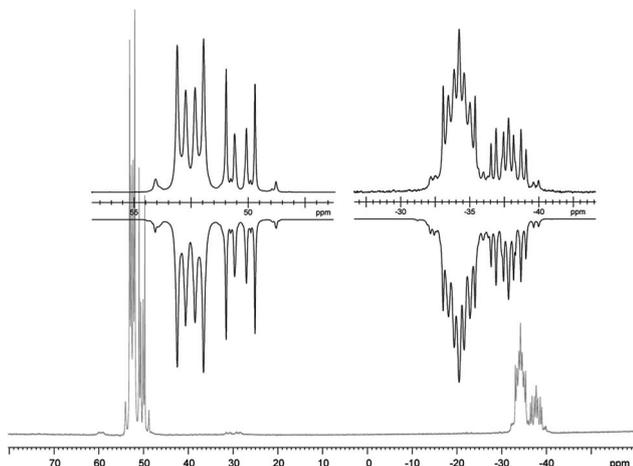
Fig. 5 ³¹P NMR spectrum of [(9a*Au)₂][OTf]₂ (CD₂Cl₂, 243 K, insets show the two AA′XX′X″X‴ spin systems of the experimental (upwards) and fitted spectra (downwards)).

also observed. However, further line splitting can be observed as a result of the complexation with the Ag¹⁰⁷/Ag¹⁰⁹ nuclei, which made us refrain from iteratively fitting the corresponding ³¹P NMR spectrum. The ³¹P NMR spectrum of the dinuclear copper complex [(9a*Cu)₂][OTf]₂ shows only the resonances of one AA′XX′X″X‴ spin system at $\delta(P_A)$ = −39.1 ppm and $\delta(P_X)$ = 15.4 ppm. An additional broadened AX₂ spin system ($\delta(P_A)$ = −37.5 ppm and $\delta(P_X)$ = 15.3 ppm ($^1J(P_AP_X)$ = −168 Hz)) gives rise to the formation of a monomeric species in solution which was not further investigated. A comparable AX₂ spin system is observed for [(9a)₂*Cu][OTf] ($\delta(P_A)$ = −44.8 ppm and $\delta(P_X)$ = −8.9 ppm ($^1J(P_AP_X)$ = −275 Hz)) as well as for (9a*CuBr)₂ ($\delta(P_A)$ = −46.6 ppm and $\delta(P_X)$ = −6.2 ppm ($^1J(P_AP_X)$ = −253 Hz)). For both mononuclear copper complexes the resonances in the ³¹P NMR spectrum are noticeably broadened due to the fast quadrupole relaxation of the ⁶³Cu nucleus.[22,23] Theoretical calculations performed at the BP86-D3/def2-TZVP level of theory support the isomerisation in the dinuclear metal complexes [(9a*M)₂]²⁺. For [(9a*Cu)₂]²⁺ we found a relative energy difference between the *syn-* and the *anti*-isomer of 5.0 kcal mol⁻¹ which explains that only one isomer is observed in the ³¹P NMR spectrum. While the two isomers of [(9a*Ag)₂]²⁺ are isoenergetic with a difference of 0.1 kcal mol⁻¹, the *syn*-isomer of

[(9a*Au)₂]²⁺ is favored by 1.7 kcal mol⁻¹ compared to its *anti*-isomer. The optimised geometries also show the different coordination behaviour of the pyridyl-moieties in the three metal complexes [(9a*M)₂]²⁺. While the free electron pair of the pyridyl nitrogen atom is pointing towards the metal centre in [(9a*Cu)₂]²⁺ and [(9a*Ag)₂]²⁺ it is pointing towards the middle of the Au–Au bond in [(9a*Au)₂]²⁺ (Fig. 4, right). Our calculations furthermore indicate that the isomerisation is not driven by rotation but proceeds *via* dissociation of the M(I)–N coordination bond or *pseudo*-coordination in the case of [(9a*Au)₂]²⁺ and subsequent association of the ligand on the opposite side (Fig. 6). This interconversion is the highest in energy for [(9a*Cu)₂]²⁺ (14.7 kcal mol⁻¹), followed by [(9a*Ag)₂]²⁺ (13.2 kcal mol⁻¹) and finally [(9a*Au)₂]²⁺ (9.6 kcal mol⁻¹).[23]

Further reactivity studies on triphosphane **9a** revealed that this compound readily rearranges in solution by means of a P–P/P–P bond metathesis reaction. After 24 h the CH₂Cl₂ solution of **9a** shows an additional singlet resonance at $\delta(P)$ = 21.0 ppm which we assign to tetracyclohexyldiphosphane (**12**)[24] and an AA′BB′C spin system at $\delta(P)$ = 14.0–25.2 ppm being characteristic of pentaphospholanes of type (RP)₅.[24,25] As this scrambling reaction is in a state of equilibrium the isolation of **13** is hampered. However, the reaction of pure **13** with Cy₄P₂ yielding **9a** illustrates that pentaphospholane **13** might be used as a PyP-synthon as it inserts into the P–P bond of Cy₄P₂. The selective synthesis of pentaphospholane **13** is achieved by the equimolar reaction of **7** with Cy₂PH in Et₂O as a non-polar solvent (Scheme 6). The formed precipitate is filtered and

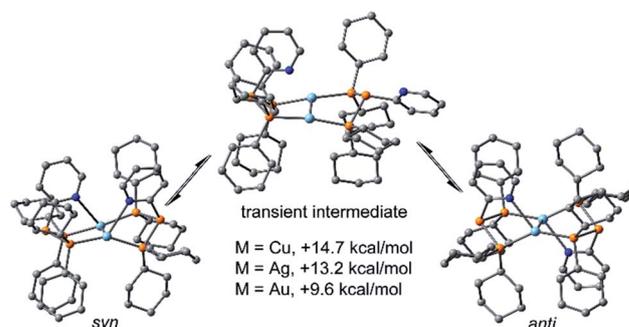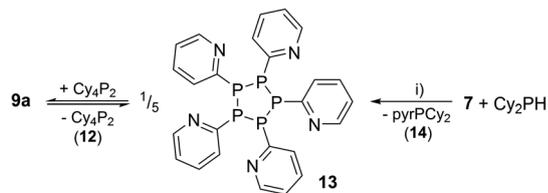**Fig. 6** Interconversion mechanism of the *syn-* and *anti*-isomers of [(9a*M)₂]²⁺; (M = Cu, Ag, and Au).

Scheme 6 Equilibrium reaction of **9a** with **13** and **12** and selective synthesis of **13** by the reaction of **7** with Cy$_2$PH; (i) Et$_2$O, −pyrH.

Fig. 8 ^{31}P NMR spectrum of the reaction of **7** with Cy$_2$PH in a 1 : 1 ratio in CD$_2$Cl$_2$ after 3.5 h; unidentified products are marked with asterisks.

dried *in vacuo* giving **13** in 98% yield as a colourless powder which shows the AA′BB′C spin system in the ^{31}P NMR spectrum (Fig. 7). Dicyclohexyl(3,5-dimethylpyrazolyl)phosphane (**14**) is identified as a side product in the supernatant solution by its singlet resonance in the ^{31}P NMR spectrum (δ(P) = 58.4 ppm) indicating a P–N/P–P bond metathesis reaction.[6] To further understand the formation of **13** we studied the reaction in CD$_2$Cl$_2$ by means of ^{31}P NMR spectroscopy (Fig. 8). After 3.5 h compound **7** is still present in the solution while Cy$_2$PH is fully consumed by the condensation reaction with **7** to form triphosphane **9a** (*vide supra*) and diphosphane **15** which is identified by an AX spin system (δ(P$_A$) = 10.2 ppm and δ(P$_X$) = 33.4 ppm; ^1J(P$_A$P$_X$) = −281 Hz). The AMX spin system at δ(P$_A$) = −35.6 ppm, δ(P$_M$) = −7.2 ppm and δ(P)$_X$ = 29.9 ppm is assigned to triphosphane **16** which is formed *via* a P–N/P–P bond metathesis reaction of two equivalents of **15** and *via* a P–N/P–P bond metathesis reaction of **7** and **9a** (Scheme 7). In both cases phosphane **14** is liberated. We propose a further chain growth in which triphosphane **16** reacts with **15** with the release of phosphane **14** in a P–N/P–P oligomerisation reaction which ultimately yields pentaphospholane **13**. We furthermore propose the formation of tetraphosphetane **17** (δ(P) = −49.4 ppm) which can be formed *via* the reaction of two equivalents **16** with concomitant release of **14** (Scheme 7). Similar to the known ring expansion reactions of certain cyclophosphanes,[26] **17** might react to form pentaphospholane **13**, being the
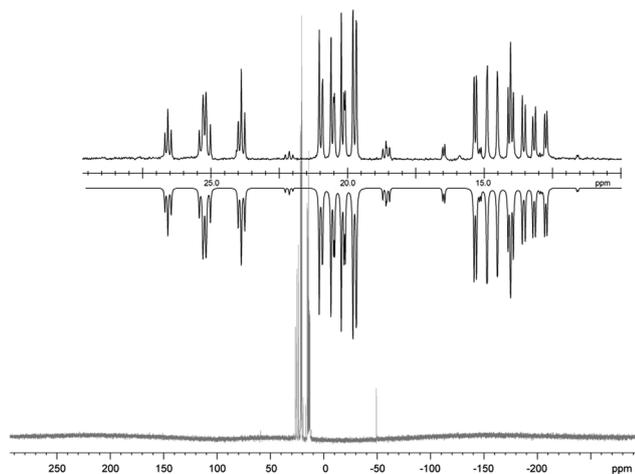
thermodynamically favoured product. In analogy to **13** we are able to isolate the corresponding benzothiazolyl substituted pentaphospholane **18**.[27] Crystals suitable for X-ray analysis are obtained for both compounds by the slow diffusion of *n*-pentane into saturated CH$_2$Cl$_2$ solutions at −30 °C (Fig. 9).

Both compounds reveal the typical envelope conformation of the P$_5$-ring featuring the substituents in the all-*trans* position. The P–P bond lengths observed for both pentaphospholanes **13** (av. P–P 2.218 Å) and **18** (av. P–P 2.246 Å) are in a range known for pentaphospholanes such as (PhP)$_5$ (av. 2.217 Å); also the P–P–P angles are in good accordance with the reported data for (PhP)$_5$.[28] We subsequently envisioned the use of **13** as a PyP-synthon for insertion reactions into P–P bonds which was already indicated by the aforementioned scrambling reaction between **9a**, Cy$_4$P$_2$ and **13** (see Scheme 6).

As similar scrambling reactions might be expected for triphosphanium and triphosphanediiium salts, we methylated triphosphane **9a** with different amounts of MeOTf. The ^{31}P

Fig. 7 ^{31}P NMR spectrum of pentaphospholane **13** (CD$_3$CN, 300 K, the inset shows the AA′BB′C spin system of the experimental (upwards) and fitted spectra (downwards)).

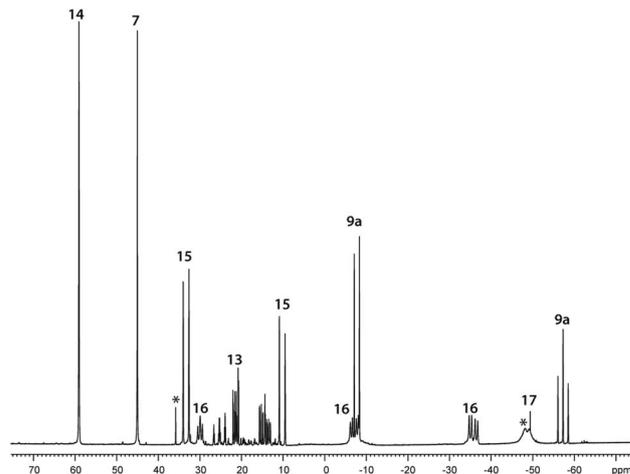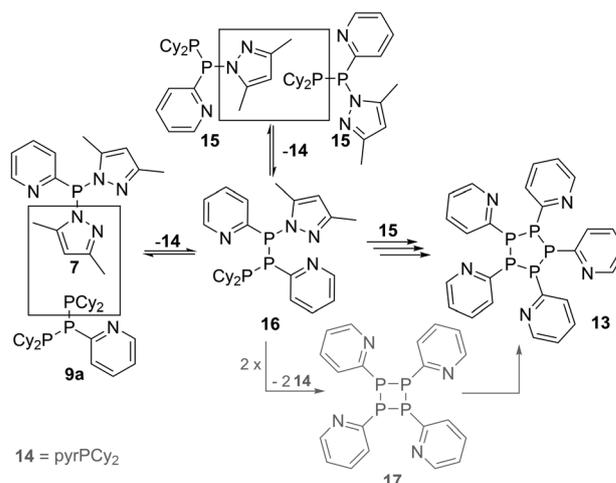**Scheme 7** Possible formation of **16** *via* P–N/P–P bond metathesis reactions.
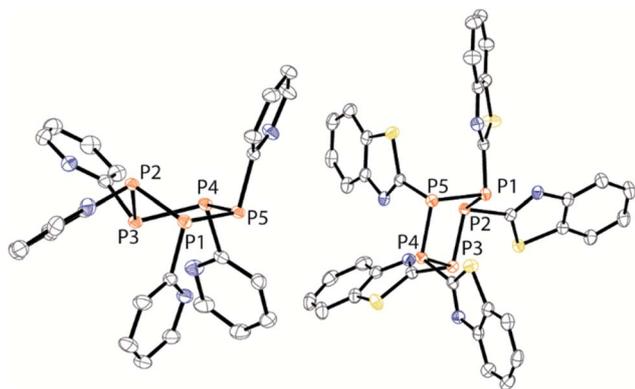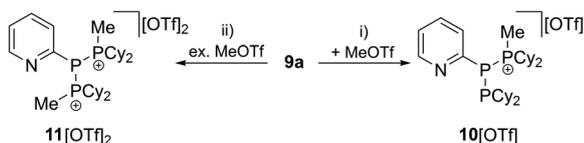
Fig. 9 Molecular structures of the pentaphospholanes **13** (left) and **18** (right) (hydrogen atoms and solvate molecules are omitted for clarity and thermal ellipsoids are displayed at 50% probability). Selected bond lengths (Å) and angles (°) (**13**): P1–P2 2.2222(4), P2–P3 2.2200(5); P3–P4 2.22200(5), P4–P5 2.2078(4), P1–P2–P3 97.25(2), P2–P3–P4 95.59(2), P3–P4–P5 102.27(2), P4–P5–P1 106.77(2), P5–P1–P2 97.14(2) (**18**); P1–P2 2.2336(6), P2–P3 2.2232(6), P3–P4 2.338(6), P4–P5 2.2069(6), P5–P1 2.2288(6), P1–P2–P3 93.54(2), P2–P3–P4 100.29(2), P3–P4–P5 107.27(2), P4–P5–P1 96.32(2), P5–P1–P2 96.85(2).
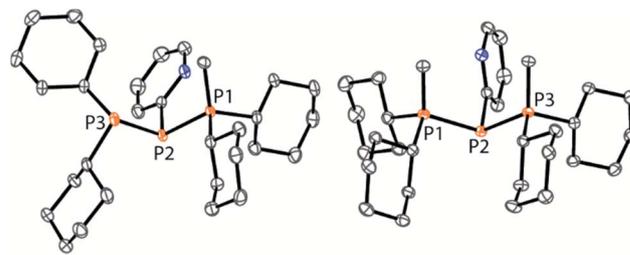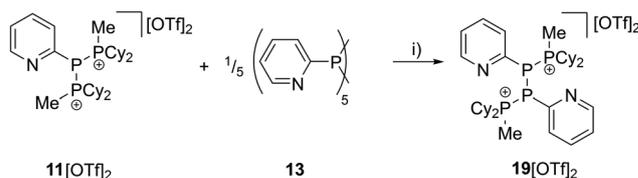

Fig. 10 Molecular structures of 10^+ in **10**[OTf] (left) and 11^{2+} in **11** [OTf]$_2$ (hydrogen atoms and anions are omitted for clarity and thermal ellipsoids are displayed at 50% probability). Selected bond lengths (Å) and angles (°) (10^+): P1–P2 2.1956(5), P2–P3 2.2362(5), P1–P2–P3 97.89(2) (11^{2+}); P1–P2 2.2152(4), P2–P3 2.2182(4), and P1–P2–P3 107.43(1).

NMR spectrum of the 1 : 1 reaction of **9a** with MeOTf shows an AMX spin system ($\delta(P_A) = -46.2$ ppm, $\delta(P_M) = -12.9$ ppm and $\delta(P_X) = 34.2$ ppm ($^1J(P_AP_M) = -290$ Hz, $^1J(P_AP_X) = -281$ Hz, and $^2J(P_MP_X) = 58$ Hz)), suggesting the methylation of the phosphorus atom rather than the nitrogen atom of the pyridyl-substituent. After the removal of all volatiles *in vacuo* triphosphan-1-ium triflate salt **10**[OTf] can be isolated in quantitative yield as a colourless powder. A second methylation is achieved when **9a** is reacted with an excess of MeOTf under solvent free conditions (Scheme 8). Similar to the aforementioned reaction, only the phosphorus atoms are methylated giving triphosphane-1,3-diiumtriflate salt **11**[OTf]$_2$. As both dicyclohexylphosphanyl moieties are methylated, the ^{31}P NMR spectrum of **10**[OTf]$_2$ shows an AX$_2$ spin system with resonances at $\delta(P_A) = -67.9$ ppm and $\delta(P_X) = 44.0$ ppm ($^1J(P_AP_X) = -315$ Hz). The molecular structures of cation 10^+ and dication 11^{2+} are depicted in Fig. 10. Note that a small number of triphosphanediium salts are reported in the literature and compound **10**[OTf] extends the library of cationic, catenated phosphorus compounds as a structurally characterised triphosphan-1-ium salt.[29–31] The P1–P2 bond length in cation 10^+ (P1–P2 2.1956(5) Å) is shortened whereas the P2–P3 bond (P2–P3 2.2362(5) Å) is comparable to those in **9a** (P1–P2 2.2301(3) Å, P1–P3 2.2371(3) Å) or similar diphosphanium cations (compare [Ph$_2$P–PPh$_3$]$^+$:

2.230(1) Å).[29b] The P–P–P bond angle in 10^+ (97.89(2)°) is similar to that in compound **9a** (97.16(6)°). The P–P bond lengths in 11^{2+} (P1–P2 2.2152(4) Å and P2–P3 2.2182(4) Å) are marginally shorter compared to those in **9a** but in accordance with bond lengths reported for similar triphosphane-1,3-diium cations (compare [Me$_3$P–P(Cy)-PMe$_3$]$^{2+}$: 2.1979(5) Å and 2.1976(6) Å).[29b] The P–P–P bond angle in 11^{2+} (107.43(1)°) is significantly wider compared to those in **9a** and [Me$_3$P–P(Cy)-PMe$_3$]$^{2+}$ (103.11(2)°). In order to investigate the envisioned PyP-transfer into a P–P bond, we reacted **13** with 5 equivalents of **11**[OTf]$_2$ in CH$_3$CN (Scheme 9). Upon addition of **13** to a colourless CH$_3$CN solution of **11**[OTf]$_2$ the reaction mixture turns from deep red to pale yellow. The ^{31}P NMR spectrum of the reaction mixture after 24 h shows two AA′XX′ spin systems which are attributed to two isomers of tetraphosphane-1,4-diium cations 19^{2+} (Fig. 11), indicating the successful PyP-transfer *via* a P–P/P–P bond metathesis reaction. The A part of the prominent AA′XX′ spin system at $\delta(P_A) = -55.1$ ppm is assigned to the inner pyridyl-substituted P nuclei and the X part at $\delta(P_X) = 40.7$ ppm to the tetra-coordinate phosphorus atoms which is similar to known tetraphosphane-1,4-diium salts.[32] The minor spin system resonates at $\delta(P_A) = -40.1$ ppm and $\delta(P_X) = 39.8$ ppm, respectively. After work-up compound **19**[OTf]$_2$ can be isolated analytically pure in 51% yield. X-ray analysis revealed that the centrosymmetric *meso*-isomer 19^{2+} crystallized showing a central torsion angle of 180° (Fig. 11). The P–P bond lengths in 19^{2+} (P1–P2 2.234(1) Å and P2–P2′2.232(2) Å) are in good agreement with the reported data for comparable tetraphosphane-1,4-diium cations (compare [Ph$_3$P–(PPh)$_2$–PPh$_3$]$^{2+}$: P1–P2 2.258(1) Å, P2–P2′ 2.221(1) Å).[32] Similar to the reported PhP-transfer from (PhP)$_5$ to a NHC,[33] **13** can be used as a PyP-synthon, thus featuring an

Scheme 8 Methylation reactions of **9a**; (i) 1 eq. MeOTf, Et$_2$O; (ii) 5 eq. MeOTf, neat.

Scheme 9 Synthesis of tetraphosphane-1,4-diium triflate salt **19** [OTf]$_2$; (i) MeCN.
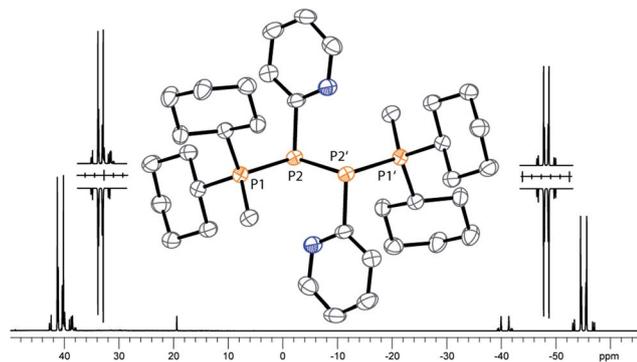
Fig. 11 ^{31}P NMR spectrum of dication 19[OTf]$_2$ (CD$_2$Cl$_2$, 300 K, the inset shows the AA'XX' spin system of the experimental (upwards) and fitted spectra (downwards)); molecular structure of 19^{2+} in 19[OTf]$_2$ (hydrogen atoms and anions are omitted for clarity; thermal ellipsoids are displayed at 50% probability). Selected bond lengths (Å) and angles (°):P1–P2 2.234(1), P2–P2' 2.232(2), and P1–P2–P2' 97.60(6).

Fig. 13   Molecular structure of 1,4,2-diazaphospholium 21$^+$ in 21[OTf] (left) and 3λ^5-triphosph-2-en-1-ium 20$^+$ in 20[OTf] (right) (hydrogen atoms and anions are omitted for clarity and thermal ellipsoids are displayed at 50% probability). Selected bond lengths (Å) and angles (°) (20$^+$): P1–C1 1.733(1), P1–N2 1.741(1), C1–P1–N2 87.08(6) (20); P1–P2 2.134(4), P2–P3 2.1382(4), P1–P2–P3 103.85(2).

additional reaction or coordination site. When compound 19[OTf]$_2$ was kept in a CD$_3$CN solution for 14 days, the ^{31}P NMR spectrum shows three rearrangement products (Fig. 12). Next to an AX$_2$ spin system ($\delta(P_A) = -235.3$ ppm and $\delta(P_X) = 38.8$ ppm ($^1J(P_AP_X) = -501$ Hz)), a *pseudo* triplet resonance ($\delta(P) = 153.1$ ppm; $^1J(PN) = 50$ Hz) and an AMXY spin system ($\delta(P_A) = -208.2$ ppm, $\delta(P_M) = -30.0$ ppm, $\delta(P_X) = 31.1$ ppm, and $\delta(P_Y) = 39.8$ ppm; $^1J(P_AP_Y) = -490$ Hz, $^1J(P_MP_X) = -342$ Hz, $^1J(P_AP_M) = -298$ Hz, $^2J(P_MP_Y) = 91$ Hz, $^2J(P_AP_X) = 45$ Hz, $^3J(P_XP_Y) = 34$ Hz) are observed. The AX$_2$ spin system can be attributed to the 3λ^5-triphosph-2-en-1-ium cation (20$^+$), as the spectroscopic parameters are in the range of those observed for [Ph$_3$P–P–PPh$_3$]$^+$ ($\delta(P_A) = -174$ ppm and $\delta(P_X) = 30$ ppm; $^1J(P_AP_X) = -500$ Hz) which was first reported by Schmidpeter and co-workers.[34] A variety of similar derivatives has been synthesised and reported by the group of Macdonald.[35] Slow vapour diffusion of Et$_2$O into the CD$_3$CN solution yielded crystals suitable for X-ray analysis confirming the structural connectivity of 20$^+$ (Fig. 13). The

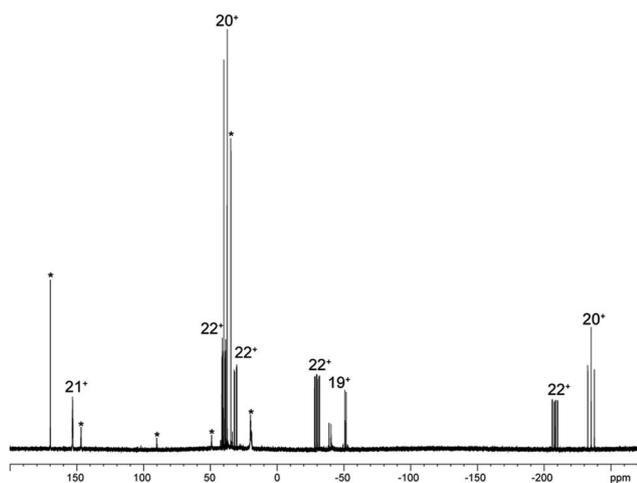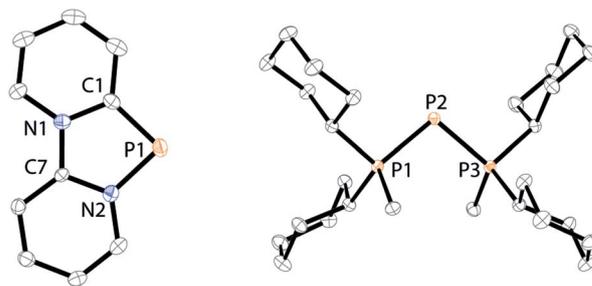structural parameters of 20$^+$ are similar to those observed for the cation [Ph$_3$P–P–PPh$_3$]$^+$, *i.e.* slightly shortened P–P bond lengths (P1–P2 2.134(4), P2–P3 2.1382(4)) and a P–P–P bond angle of 103.85(2)°.[34] By co-crystallisation, a further product was identified as the triflate salt of diazaphospholium cation 21$^+$ (Fig. 13). We assign this species to the *pseudo* triplet resonance observed in the ^{31}P NMR spectrum. The P–C bond distance of 1.733(1) Å slightly exceeds the upper limit of typical P=C bond lengths (1.61–1.71 Å),[36] while the P–N bond length of P1–N2 1.741(1) Å indicates a P–N single bond (P–N: 1.78 Å).[37] Furthermore, the structure of 21$^+$ reveals an acute angle around the P atom (C1–P1–N2 87.08(6)°) and a planar arrangement, suggesting a delocalized π-system. We assign the AMXY spin system to asymmetric tetra-phosphanediium dication 22^{2+}, most likely formed by an intra-molecular aromatic substitution reaction of 19^{2+}. This can be attributed to be the first step of the rearrangement reaction of 19^{2+} to form 20$^+$ and 21$^+$. We further studied this rearrangement reaction using the TURBOMOLE 7.0 program at the PB86-D3/def2-TZVP level of theory (see ESI for details†) and taking into consideration solvent effects by using the Conductor-like Screening Model (COSMO). Our calculations started from 22$^+$ and show that the cleavage of Cy$_2$PMe is energetically quite costly. This is in accordance with the ^{31}P NMR spectrum as Cy$_2$PMe is not observed ($\delta(P) = -19.8$ ppm).[38] More likely and energetically favoured is a [1,2]-shift of the Cy$_2$PMe group to form iso-22^{2+} with a reaction barrier of +22.0 kcal mol^{-1}. Fig. 14 shows the opti-mised structures for this [1,2]-Cy$_2$PMe shift reaction. It is note-worthy that similar [1,2]- and [1,3]-PR$_3$ shifts have been reported.[39] Compared to 22^{2+}, iso-22^{2+} is almost isoenergetic and

Fig. 12 ^{31}P NMR spectrum of a solution of 19[OTf]$_2$ in CD$_3$CN after 14 days.
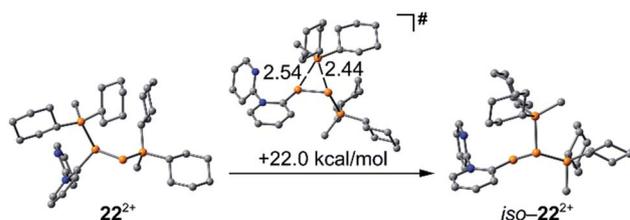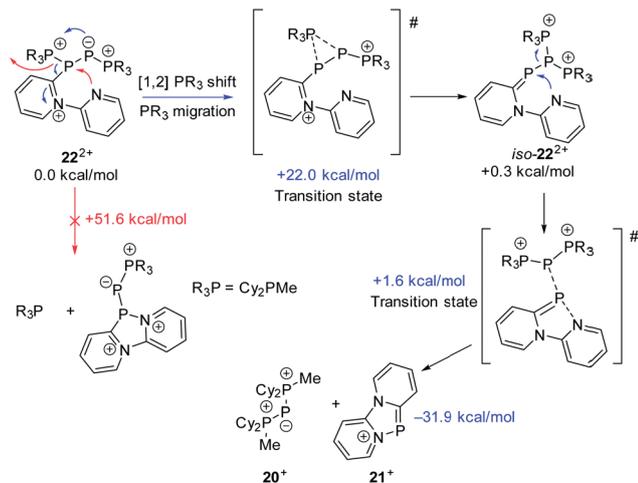

Fig. 14   Optimised structures of 22^{2+}, iso-22^{2+} and the transition state.

Scheme 10 Rearrangement reaction of 22^{2+} to 20^+ and 21^+ calculated at the PB86-D3/def2-TZVP level of theory.

readily reacts in an exergonic step (-31.9 kcal mol^{-1}) to form cations 20^+ and 21^+ with a low barrier of only 1.9 kcal mol^{-1} (see Scheme 10 and ESI for details†).

Conclusions

In summary we have shown that phosphanes which we denote as type II phosphanes (two P–N bonds and one P–C bond) can be used to build polyphosphorus compounds featuring a further nitrogen donor functionality at the C bound substituent. The reactions of type II phosphanes **7** and **8** with secondary phosphanes of type R′$_2$PH in a 1 : 2 ratio in MeCN give triphosphanes **9a–c** and triphospholane **9d** via protolysis reactions. With the multi-gram scale synthesis of **9a** we were able to conveniently investigate its coordination chemistry towards coinage metal salts. The synthesised coordination complexes are studied by X-ray analysis, multi nuclear NMR spectroscopy and quantum chemical calculations. Further reactivity studies of **9a** focused on the reaction with the electrophilic MeOTf. Depending on the amount of MeOTf, the reaction yields triphosphane-1,3-diium triflate salt **11**[OTf]$_2$ or triphosphan-1-ium **10**[OTf] featuring a hitherto unknown structural motif. Pentaphospholanes **13** and **18** are synthesised by reacting type II phosphane **7** or **8** with Cy$_2$PH in a 1 : 1 ratio in Et$_2$O or CH$_2$Cl$_2$, respectively. The reaction proceeds via a controlled scrambling reaction showing the susceptible solvent dependency of the reaction of **7** and **8** with Cy$_2$PH. By reacting **11**[OTf]$_2$ with **13** we have shown that pentaphospholane **13** is a suitable PyP-synthon in a P–P/P–P bond metathesis reaction to yield tetraphosphane-1,4-diium triflate **19**[OTf]$_2$. In an interesting rearrangement reaction **19**[OTf]$_2$ forms triphosph-2-en-1-ium triflate salt **20**[OTf] and 1,4,2-diazaphospholium triflate **21**[OTf] via an unprecedented [1,2]-Cy$_2$MeP shift. Based on our findings we are certain that controlled P–N(P)/P–P bond metathesis reactions will allow us to access larger acyclic and cyclic polyphosphanes in

a controlled stepwise manner in order to further investigate their fascinating reaction space.

Conflicts of interest

There are no conflicts to declare.

Acknowledgements

Notes and references

1 M. Donath, F. Hennersdorf and J. J. Weigand, *Chem. Soc. Rev.*, 2016, **45**, 1145; M. H. Holthausen and J. J. Weigand, *Chem. Soc. Rev.*, 2014, **43**, 6639; S. Gomez-Ruiz and E. Hey-Hawkins, *Coord. Chem. Rev.*, 2011, **255**, 1360; M. Scheer, G. Balazs and A. Seitz, *Chem. Rev.*, 2010, **110**, 4236; M. Baudler, *Angew. Chem., Int. Ed. Engl.*, 1987, **26**, 419.

2 (a) M. Baudler, *Angew. Chem., Int. Ed. Engl.*, 1982, **21**, 492; M. Baudler and K. Glinka, *Chem. Rev.*, 1993, **93**, 1623. ; M. Baudler and K. Glinka, *Chem. Rev.*, 1994, **94**, 1273. (b) M. Scheer, St. Gremler, E. Herrmann, U. Grünhagen, M. Dargatz and E. Kleinpeter, *Z. Anorg. Allg. Chem.*, 1991, **600**, 203; M. Scheer, St. Gremler, E. Herrmann, M. Dargatz and H.-D. Schädler, *Z. Anorg. Allg. Chem.*, 1992, **619**, 1047. (c) G. Fritz, *Comments Inorg. Chem.*, 1982, **6**, 329; G. Fritz, *Adv. Inorg. Chem.*, 1987, 171; (d) L. Maier, *Helv. Chim. Acta*, 1966, **49**, 1119; E. Niecke, R. Rüger and B. Krebs, *Angew. Chem., Int. Ed. Engl.*, 1982, **21**, 544; A. B. Burg, *J. Am. Chem. Soc.*, 1961, **83**, 2226; K. Jurkschat, C. Mugge, A. Tzschach, W. Uhlig and A. Zschunke, *Tetrahedron Lett.*, 1982, **23**, 1345.

3 M. Baudler, G. Reuschenbach and J. Hahn, *Z. Anorg. Allg. Chem.*, 1981, **482**, 27; G. Fritz and T. Vaahs, *Z. Anorg. Allg. Chem.*, 1987, **553**, 85.

4 A. H. Cowley and D. S. Dierdorf, *J. Am. Chem. Soc.*, 1965, **87**, 6609; L. R. Avend, R. A. Wolcott, L. V. Cribbs and J. L. Mills, *Inorg. Chem.*, 1989, **28**, 200; L. R. Avens, L. V. Cribbs and J. L. Mills, *Inorg. Chem.*, 1989, **28**, 211.

5 K.-O. Feldmann, R. Fröhlich and J. J. Weigand, *Chem. Commun.*, 2012, **48**, 4296.

6 K.-O. Feldmann and J. J. Weigand, *J. Am. Chem. Soc.*, 2012, **134**, 15443.

7 (a) X. Chen, H. Zhu, T. Wang, C. Li, L. Yan, M. Jiang, J. Liu, X. Sun, Z. Jiang and Y. Ding, *J. Mol. Catal. A: Chem.*, 2016, **414**, 37; (b) I. V. Komarov, A. V. Strizhak, M. Y. Kornilov, E. Zraudnitskiy and A. A. Tolmachev, *Synth. Commun.*, 2000, **30**, 243.

8   We developed a convenient, salt free synthesis of **5** and **6** which is described in the ESI.†

9   (*a*) S. Fischer, L. K. Peterson and J. F. Nixon, *Can. J. Chem.*, 1974, **52**, 3981; (*b*) S. Fischer, J. Hoyano and L. K. Peterson, *Can. J. Chem.*, 1976, **54**, 2710.

10 H. Goldwhite, *Introduction to phosphorus chemistry*, Cambridge University Press, Cambridge, 1981.

11 R. E. Cobbledick and F. W. B. Einstein, *Acta Crystallogr.*, 1975, **B31**, 2731.

12 J. J. Daly, *J. Chem. Soc. A*, 1966, 1020.

13 S. Gomez-Ruiz and E. Hey-Hawkins, *Coord. Chem. Rev.*, 2011, **255**, 1360; *Phosphorus Chemistry: Catalysis and Material Science Applications*, ed. M. Peruzzini and L. Gonsalvi, Springer, vol. 37, 2011.

14 J. W. Dube, C. L. B. Macdonald and P. Ragogna, *Angew. Chem., Int. Ed.*, 2012, **51**, 13026; J. W. Dube, C. L. B. Macdonald, B. D. Ellis and R. Paul, *Inorg. Chem.*, 2013, **52**, 11438.

15 M. Scheer, C. Kuntz, M. Stubenhofer, M. Zabel and A. Y. Timoshkin, *Angew. Chem., Int. Ed.*, 2010, **49**, 188; M. Baacke, S. Morton, G. Johannsen, N. Weferling and O. Stelzer, *Chem. Ber.*, 1980, **113**, 1328; W. S. Sheldrick, S. Morton and O. Stelzer, *Z. Anorg. Allg. Chem.*, 1981, **475**, 232; M. Scheer, S. Gremler, E. Herrmann and P. G. Jones, *J. Organomet. Chem.*, 1991, **414**, 337.

16 D. R. Armstrong, N. Feeder, A. D. Hopkins, M. J. Mays, D. Moncrieff, J. A. Wood, A. D. Woods and D. S. Wright, *Chem. Commun.*, 2000, 2483.

17 C. E. Averre, M. P. Coles, I. R. Crossley and I. J. Day, *Dalton Trans.*, 2012, **41**, 278.

18 For a review on argentophilic interactions see: H. Schmidbaur and A. Schier, *Angew. Chem., Int. Ed.*, 2015, **54**, 746, for aurophilic interactions see: H. Schmidbaur and A. Schier, *Chem. Soc. Rev.*, 2012, **41**, 370.

19 A. Bondi, *J. Phys. Chem.*, 1964, **68**, 441.

20 C.-M. Che, Z. Mao, V. M. Miskowski, M.-C. Tse, C.-K. Chan, K.-K. Cheung, D. L. Phillips and K.-H. Leung, *Angew. Chem., Int. Ed.*, 2000, **39**, 4084; C.-M. Che, M.-C. Tse, M. C. W. Chan, K.-K. Cheung, D. L. Phillips and K.-H. Leung, *J. Am. Chem. Soc.*, 2000, **122**, 2464; C.-M. Che, W.-F. Wu, K.-C. Chan and K.-K. Cheung, *Chem.–Eur. J.*, 2001, **7**, 4656.

21 M. Henary, J. L. Wootton, S. I. Khan and J. I. Zink, *Inorg. Chem.*, 1997, **36**, 796; P. Aslanidis, P. J. Cox, S. Divanidis and A. C. Tsipis, *Inorg. Chem.*, 2002, **41**, 6875.

22 H. Friebolin, *Ein- und Zweidimensionale NMR-Spektroskopie*, Wiley VCH, Weinheim, 2006; H. Fujii, M. Tomura, T. Kurahashi and M. Kujime, *Inorg. Chem.*, 2007, **46**, 541.

23 (*a*) The ^{31}P NMR spectra of [(**9a*****Cu**)$_2$][OTf]$_2$, [(**9a*****Ag**)$_2$][OTf]$_2$, [(**9a*****Au**)$_2$][OTf]$_2$, [(**9a**)$_2$***Cu**][OTf] and (**9a*****CuBr**)$_2$ are depicted in the ESI (Fig. 1–5†); (*b*) Further information on the theoretical calculations on [(**9a*****M**)$_2$][OTf]$_2$ is also given in the ESI in chapter 4.†

24 K. Schwedtmann, R. Schoemaker, F. Hennersdorf, A. Bauzá, A. Frontera, R. Weiss and J. J. Weigand, *Dalton Trans.*, 2016, **45**, 11384.

25 (*a*) J. P. Albrand, D. Gagnaire and J. B. Robert, *J. Am. Chem. Soc.*, 1973, **95**, 6498; (*b*) J. P. Albrand and J. B. Robert, *J. Chem. Soc., Chem. Commun.*, 1974, 644; (*c*) L. R. Smith and J. L. Mills, *J. Chem. Soc., Chem. Commun.*, 1974, **20**, 808.

26 (*a*) M. Baudler, J. Hahn and E. Clef, *Z. Naturforsch.*, 1984, **39b**, 438; (*b*) K. Schwedtmann, J. Haberstroh, S. Roediger, A. Bauzá, A. Frontera, F. Hennersdorf and J. J. Weigand, *Chem. Sci.*, 2019, **10**, 6868.

27 For further details see the ESI.†

28 J. J. Daly, *J. Chem. Soc.*, 1964, 6147.

29 (*a*) N. Burford, T. S. Cameron and P. J. Ragogna, *J. Am. Chem. Soc.*, 2001, **123**, 7947; (*b*) P. A. Gray, Y.-Y. Carpenter, N. Burford and R. McDonald, *Dalton Trans.*, 2016, **45**, 2124.

30 For a review on interpnictogen cations see: A. P. M. Robertson, P. A. Gray and N. Burford, *Angew. Chem., Int. Ed.*, 2014, **53**, 6050.

31 For cationic, cyclic polyphosphorus compounds see: J. Bresien, K. Faust, A. Schulz and A. Villinger, *Angew. Chem., Int. Ed.*, 2015, **54**, 6926; S. J. Geier, M. A. Dureen, E. Y. Ouyang and D. W. Stephan, *Chem.–Eur. J.*, 2010, **16**, 988; Y.-Y. Carpenter, N. Burford, M. D. Lumsden and R. McDonald, *Inorg. Chem.*, 2011, **50**, 3342; J. J. Weigand, N. Burford, R. J. Davidson, T. S. Cameron and P. Seeheim, *J. Am. Chem. Soc.*, 2009, **131**, 17943; C. A. Dyker, N. Burford, G. Menard, M. D. Lumsden and A. Decken, *Inorg. Chem.*, 2007, **46**, 4277; N. Burford, C. A. Dyker, M. Lumsden and A. Decken, *Angew. Chem.*, 2005, **117**, 6352.

32 (*a*) C. A. Dyker, N. Burford, M. D. Lumsden and A. Decken, *J. Am. Chem. Soc.*, 2006, **128**, 9632; (*b*) Y.-Y. Carpenter, C. A. Dyker, N. Burford, M. D. Lumsden and A. Decken, *J. Am. Chem. Soc.*, 2008, **130**, 15732.

33 (*a*) A. J. Arduengo III, H. V. R. Dias and J. C. Calabrese, *Chem. Lett.*, 1997, 143; (*b*) A. J. Arduengo III, J. C. Calabrese, A. H. Cowley, H. V. R. Dias, J. R. Goerlich, W. J. Marshall and B. Riegel, *Inorg. Chem.*, 1997, **36**, 2151; (*c*) J. H. Barnard, P. A. Brown, K. L. Shuford and C. D. Martin, *Angew. Chem., Int. Ed.*, 2015, **54**, 12083.

34 A. Schmidpeter, S. Lochschmidt and W. S. Sheldrick, *Angew. Chem.*, 1985, **97**, 214.

35 B. D. Ellis, M. Carlesimo and C. L. B. Macdonald, *Chem. Commun.*, 2003, 1946; B. D. Ellis and C. L. B. Macdonald, *Inorg. Chem.*, 2006, **45**, 6864; E. L. Norton, K. L. S. Szekely, J. W. Dube, P. G. Bomben and C. L. B. Macdonald, *Inorg. Chem.*, 2008, **47**, 1196.

36 M. Regitz and O. J. Scherer, *Multiple Bonds and Low Coordination in Phosphorus Chemistry*, Georg Thieme Verlag Thieme Medical Publishers, New York, 1990.

37 H. R. Allcock, *Phosphorus-Nitrogen Compounds*, Academic Press, New York, 1972.

38 E. Payet, A. Auffrant, X. F. Le Goff and P. Le Floch, *J. Organomet. Chem.*, 2010, **695**, 1499.

39 E. Rüba, K. Mereiter, R. Schmid, V. N. Sapunov, K. Kirchner, H. Schottenberger, M. J. Calhorda and L. F. Veiros, *Chem.–Eur. J.*, 2002, **8**, 3948; C. Coletti, L. Gonsalvi, A. Guerriero, L. Marvelli, M. Peruzzini, G. Reginato and N. Rem, *Organometallics*, 2010, **29**, 5982.